

Two-Phase Approach to High-Quality, Oil-Soluble, Near-Infrared-Emitting PbS Quantum Dots by Using Various Water-Soluble Anion Precursors

Dawei Deng,^[a,b] Jie Cao,^[b] Junfei Xia,^[b] Zhiyu Qian,^[c] Yueqing Gu,^{*,[b]} Zhongze Gu,^{*,[a]} and Walter John Akers^[d]

Keywords: Lead sulfide / Quantum dots / Synthesis design / Fluorescence

Colloidal PbS quantum dots (QDs) with tunable photoemission throughout the near-infrared (NIR) region (ca. 750–1000 nm) were synthesized by a two-phase approach. Here, oil-soluble lead oleate formed by a reaction of lead acetate and oleic acid (OA, the capping agent) in *n*-decane at 130 °C was used as lead precursor, and water-soluble Na₂S, thioacetamide (TAA), and thiourea, each having a different reactivity, were used as sulfur sources. When an *n*-decane solution of lead precursor and an aqueous solution of sulfur pre-

cursor were mixed at the appointed temperature, oil-soluble, near-infrared-emitting PbS QDs were achieved. In this study, we investigated the influence of the reactivity of water-soluble sulfur sources on the synthesis of PbS QDs. The morphology and crystal structure of the as-prepared PbS QDs were characterized by (high-resolution) transmission electron microscopy (TEM), selected area electron diffraction (SAED), and X-ray diffraction (XRD).

Introduction

Colloidal semiconductor quantum dots (QDs, or nanocrystals) have attracted tremendous attention since the 1990s, owing to their unique size-dependent optical and electronic properties,^[1] as well as their potentials for applications in light-emitting diodes (LEDs), solar cells, and biological labeling.^[2] To date, a large variety of high-quality semiconductor quantum dots such as CdSe, CdTe, CdS, have been synthesized, through traditional organometallic or aqueous methods.^[3,4] Among them, colloidal QDs with tunable near-infrared (NIR) emission in the range 700–1000 nm are becoming increasingly attractive in the last five years, because they can be used for noninvasive in vivo biomedical imaging.^[5,6] The use of NIR (700–1000 nm) light for biomedical imaging is grounded in first principles, and it is best understood in the context of photon propagation through living tissue and the signal-to-background ratio (in this spectral region, the autofluorescence and absorption from most flesh tissues are lowest).^[5–7] In comparison to

commonly used organic NIR dyes, these quantum dots show many favorable photophysical properties, such as fluorescence emission that can be tuned by varying the size and composition, broad excitation spectra, large Stokes shifts, and superior photostability.^[5] QDs have therefore been promising alternatives to organic NIR dyes in many applications.^[5,6] Thus, the synthesis of inorganic QDs emitting in the NIR, the optical window for in vivo imaging, is of particular interest.

Over the past decade, great efforts have been invested into the synthesis of NIR-emitting QDs.^[5,6] On the basis of CdTe (typically, type II CdTe/CdSe),^[8,9] CdHgTe,^[10] and HgTe^[11] semiconductors, quantum dots emitting above 700 nm in the NIR region were firstly obtained. Unfortunately, these Cd-, Hg-, Te-, and Se-based quantum dots show high in vitro and in vivo toxicity, since they will eventually lead to a release of toxic elements (compounds).^[12] This represents a major roadblock to the practical use of QDs and has motivated the development of new Hg- and Cd-free NIR QDs, based on III–V,^[12–14] I–III–VI₂,^[15–18] or other semiconductors, such as representative InAs,^[12,13] InP,^[14] CuInSe₂,^[16] CuInS₂,^[17] and so on.^[18] However, so far, most of the previous approaches are, to the best of our knowledge, still very complicated and need high reaction temperatures (greater than ca. 200 °C).^[12–18] Furthermore, there are some other major problems that are worth mentioning. For InP and InAs nanocrystals,^[12–14] the precursors, namely tris(trimethylsilyl) phosphide and tris(trimethylsilyl) arsenide, are extremely expensive, unstable, and hazardous; the resulting phosphides and arsenides exhibit poor chemical stability in comparison to sulfides, which is always a concern in technical applications. For Cu-

[a] State Key Laboratory of Bioelectronics, School of Biological Science and Medical Engineering, Southeast University, Nanjing 210096, China
E-mail: gu@seu.edu.cn

[b] Department of Biomedical Engineering, School of Life Science and Technology, China Pharmaceutical University, Nanjing 210009, China

[c] Department of Biomedical Engineering, School of Automation, Nanjing University of Aeronautics and Astronautics, Nanjing 210016, China
E-mail: cpuyueqing@163.com

[d] Department of Radiology, Washington University School of Medicine, 4525 Scott Ave, St. Louis, USA

InSe₂ and CuInS₂ nanocrystals, not surprisingly, control of the ternary composition stoichiometric ratio in the nanocrystals is an obvious challenge, in comparison to binary semiconductor nanocrystals; to prevent the oxidation of copper(I) in nanocrystals and improve the optical properties, forming the CuInS₂(or CuInSe₂)/ZnS core/shell structure is essential, through complex high-temperature processes.^[15–17] Hence, developing a new, facile, rapid, and mild approach to synthesize air-stable NIR-emitting QDs remains an urgent challenge for scientists.

Compared with the materials mentioned above, PbS can offer notably excellent size tunability across in the NIR region, in view of its small band gap (0.41 eV) and large exciton Bohr radius (18 nm).^[19] Meanwhile, it also provides a chance to produce air-stable, NIR-emitting QDs with inexpensive and relatively safe synthesis precursors.^[19] Here we focus on the controlled synthesis of luminescent colloidal PbS QDs. In previous reports, most of the synthesis efforts have been made on synthesizing irregularly shaped PbS nanocrystals;^[20] only a limited number of approaches have been used to form spherical PbS QDs, in aqueous or organic media.^[19,21–26] For water-soluble PbS QDs, prepared firstly by Kumacheva et al.,^[21] lead acetate and sodium sulfide were used as reactant sources, while thioglycerol and dithioglycerol were added as capping agents. However, as indicated in our recent report,^[22] the resulting aqueous PbS QDs exhibited long-wavelength emission ranging from 1000 to 1400 nm,^[21] relatively poor storage stability, and low photoluminescence (PL) quantum efficiency (ca. 10%), although these water-soluble approaches are very facile.^[21–23] For non-water-soluble (or oil-soluble) PbS QDs,^[19] the hot-injection approach developed by Hines and Scholes seems to be the best to engineer high-quality QD ensembles. This hot-injection method was conducted by heating a mixture of lead oxide (PbO) and oleic acid (OA, as capping ligands) in octadecene (ODE) at 150 °C under Ar for one hour followed by the injection of a solution of (TMS)₂S (sulfur source) in ODE at 150 °C. After the hot injection, the QD growth was monitored either at 80–140 °C or at room temperature. The resulting oil-soluble PbS QDs exhibited long-wavelength emission in the range 1000–2000 nm (PL quantum yield: ca. 20%), presumably due to the high hot-injection temperature.^[19,24] Subsequently, the optical properties of oil-soluble PbS QDs were further optimized through the hot injection method and its variants.^[19,24–26] Very recently, the group of Yu developed a new non-injection approach to synthesize NIR-emitting PbS QDs in ODE.^[27] These results represented the best optical quality of the NIR fluorescent PbS QDs in organic media. However, unfortunately, these methods are still complicated and involve the dangerous chemical bis(trimethylsilyl) sulfide [(TMS)₂S] or poorly reactive elemental S.

As described above, these previous reactions were all carried out either in the aqueous phase or the organic phase, and both nucleation and growth of the QDs happened only in a homogeneous system.^[19,21–27] As expected, if we can combine the respective advantages of both approaches properly, for instance, to synthesize oil-soluble QDs by

using water-soluble anion precursors, the synthesis steps of the traditional organic-phase methods will be simplified greatly. However, this has proved to be a difficulty.^[28] A few years ago, the group of An succeeded in developing a versatile two-phase approach to synthesize highly luminescent CdS,^[29] extremely small CdSe,^[30] TiO₂,^[31] and other nanocrystals,^[32] derived from the Brust method.^[33] Subsequently, they further studied the nucleation and growth of CdSe and CdS QDs in a two-phase system using water-soluble Na₂S, thiourea, NaHSe, and selenourea as sulfur and selenium sources.^[34] These previous studies have proven that the reactivity of water-soluble anion precursors plays an important role in affecting the nucleation and growth of the oil-soluble CdS and CdSe QDs. To the best of our knowledge, the use of the two-phase approach to synthesize NIR-emitting PbS QDs has not yet been reported, and the growth rate of PbS QDs is significantly different from those of CdS and CdSe QDs: the growth of PbS QDs is much faster, and could even occur at room temperature.^[26,27] Thus, it is of great interest to investigate and better understand what role the activity of anion precursors plays in the nucleation and growth processes of PbS QDs in a two-phase system and how to adjust the properties of the products.

In this paper, we prepared high-quality, oil-soluble PbS QDs emitting in the NIR region of 750–1000 nm by a two-phase approach for the first time and explored the influence of the reactivity of water-soluble anion precursors on the nucleation and growth processes of PbS QDs, by using Na₂S, TAA, and thiourea, which differ in reactivity, as sulfur sources. In addition, using highly reactive Na₂S as sulfur source, we investigated further the effects of the heating temperature, the precursor Pb/S molar ratio, the precursor OA/Pb molar ratio, and the storage time on the PbS synthesis, as well as studying intensively the role of the reaction temperature in controlling the reactivity of water-soluble anion precursor, by using moderately reactive TAA as sulfur source. The progress achieved by this two-phase approach not only increases the quality of these oil-soluble PbS QDs, especially their emissive properties, up to a level comparable to that of CdSe and other II–VI semiconductor QDs, but also enhances our understanding of the relation between the reactivity of water-soluble anion precursors and the synthesis of oil-soluble QDs in a two-phase system.

Results and Discussion

This manuscript addresses our two-phase approach to NIR-emitting, oil-soluble PbS QDs in *n*-decane, by using differently reactive water-soluble Na₂S and thioacetamide (and thiourea) as sulfur precursors. The results and discussion are presented in two main parts. The QD synthesis using highly reactive Na₂S as sulfur precursor is presented first. Here, various synthesis parameters affecting the quality of the PbS QDs are discussed in detail, in the sequence heating temperature, precursor Pb/S molar ratio, precursor OA/Pb molar ratio, and storage time. The QD synthesis with moderately reactive thioacetamide (and poorly reactive

thiourea) as sulfur precursor is dealt with next, and here the influence of the reaction temperature on the nucleation and growth of PbS QDs is investigated intensively. In addition, we also present the results of the further characterization of the morphology and crystal structure of the as-prepared PbS QDs by means of TEM, SAED, and powder XRD.

Synthesis of OA-Capped PbS QDs with Highly Reactive Na_2S as Sulfur Source

In this study, we initially used the highly reactive Na_2S as sulfur precursor to synthesize OA-capped PbS QDs by a two-phase method. The typical synthesis steps are described in the Experimental Section. When the aqueous solution of Na_2S was added dropwise to the lead oleate precursor solution whilst stirring, the color of the upper organic phase changed from clear yellow to dark-brown instantly, indicating the formation of PbS QDs. Figure 1 shows the absorption and PL spectra of the as-prepared OA-capped PbS QDs with an OA/Pb/S molar ratio of 40:10:3. The absorption shoulder and PL peak are at 595 and 770 nm, respectively. Compared with bulk PbS (the band gap energy for bulk-phase PbS is 0.41 eV; $\lambda_{\text{max}} = 3020$ nm), the PL peak and absorption shoulder are vastly blueshifted. Thus, the band gap of PbS QDs is engineered in the near-infrared spectral region of 700–900 nm, which is also evidence for the strong effect of quantum confinement. Clearly, the photoemission bandwidth is narrow, with full width at half-maximum (fwhm) on the order of approximately 100 nm. Here, it is worth noting that this fwhm value is small and comparable to the best values obtained with other synthesis routes,^[19,21–27] which suggests a narrow size distribution achieved without any post-synthesis size-selective precipitation (Figure 7 <xigr7>A). Also, the PL quantum yield (QY) of the resulting oil-soluble PbS QDs in *n*-decane was estimated to be approximately 30% (relative to the NIR dye cypate in 20% aq. DMSO). To the best of our knowledge, this PL QY is larger than those previously reported (PL QY ca. 20%),^[24–27] especially those obtained in water solution (PL QY ca. 10%).^[21–23]

In addition to these advantages, the present two-phase approach is more facile and environmentally friendly, because of the use of the low-cost, less noxious, and highly reactive water-soluble Na_2S as sulfur precursor, relative to the existing organic routes based on bis(trimethylsilyl) sulfide $[(\text{TMS})_2\text{S}]$, sulfur source.^[19,24,27] As we know, the chemical $(\text{TMS})_2\text{S}$ is dangerous, toxic, and expensive. With poorly reactive elemental S ,^[25] higher reaction temperatures (90–220 °C) are needed, and the resulting PbS QDs exhibit long-wavelength emission in the range approximately 1250–1500 nm. Hence, using water-soluble Na_2S as sulfur source is very favorable for the preparation of high-quality, oil-soluble PbS QDs with tunable emission in the NIR optical window of approximately 700–1000 nm, which makes these QDs more promising in near-infrared biomedical imaging.

When using highly reactive water-soluble Na_2S as sulfur source, a burst of nucleation occurred with a very fast QD

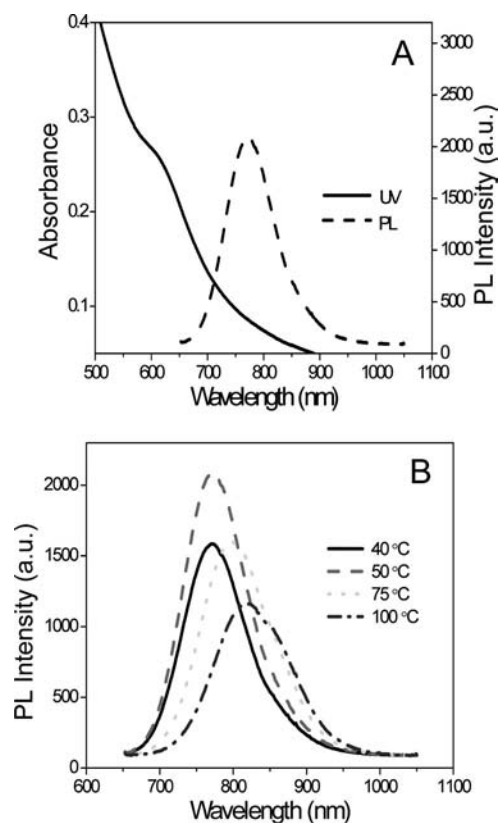


Figure 1. (A) Absorption and PL spectra of OA-capped PbS QDs using highly reactive Na_2S as sulfur precursor, where the precursor OA/Pb/S molar ratio was set to 40:10:3 ($[\text{Pb}^{2+}] = 10$ mM); (B) evolution of PL spectra of the growing PbS QDs with the reaction temperature increased from the initial synthesis temperature (40 °C) to 100 °C.

formation process, which was finished within about one minute after the complete addition of Na_2S solution, as evidenced by an immediate color change from clear yellow to dark-brown in the reaction vessel. To promote further growth of PbS QDs in this study, the reaction flask was heated up by a rate of approximately 2 °C/min. Aliquots were taken at 40, 50, 75, and 100 °C during the heat treatment. Each sample aliquot was kept in a vial and cooled down to room temperature. Figure 1B shows the evolution of the PL spectra of the growing PbS QDs with the reaction temperature. During such a temperature increase, the PL peak of the resulting PbS QDs redshifts from approximately 770 to about 823 nm, indicating the gradual growth in QD size as the temperature increases; the fwhm increases from about 105 nm to about 127 nm, which is consistent with Ostwald ripening, the process by which larger particles grow at the expense of smaller ones; the PL emission intensity reaches a maximum at 50 °C (the corresponding PL quantum yield in *n*-decane is ca. 40%), and then, it decreases gradually. If the growth temperature was further increased to 120 °C, the PL peak could redshift to approximately 860 nm, whereas the PL emission intensity would become very weak.

Optimization of the Synthesis Conditions

We explored further the influence of various synthesis parameters on the PL properties of the as-prepared PbS QDs. The obtained experimental results are presented in detail in the following sequence: the precursor Pb/S molar ratio, the precursor OA/Pb molar ratio, and the storage time. Figure 2A shows the PL spectra of OA-capped PbS QDs obtained by changing the Pb/S feed molar ratio, where the concentrations of OA and Pb^{2+} ions were fixed at 40 mM and 10 mM, respectively, and only the added amount of Na_2S was varied. When the Pb/S molar ratio was tuned from 10:1 to 10:8, the PL emission peak redshifted gradually from approximately 750 to about 880 nm. The PL intensity reached a maximum at a Pb/S molar ratio of 10:3. When the amount of Na_2S was increased further, the PL intensity decreased gradually. The experimental results (i.e., the gradual redshift of the emission peak induced by continuously feeding more Na_2S) may indicate that in the present synthesis system, a section of the newly formed PbS by the reaction between the successively introduced sulfur anions and lead ions would deposit on the surface of the initially formed small QDs, resulting in an increase in the size of the QDs (as we know, the PL emission maximum of QDs is mainly determined by the particle size of the QDs).^[1–5] In addition, the Pb-rich facets of PbS QDs were capped by OA molecules as a result of the coordination interaction between the carboxyl groups of OA (ligand) and Pb cations; it can be argued that low Pb/S feed molar ratios would lower the density of lead cations existing on the surface of the PbS QDs, which would prevent the formation of a high-quality Pb–OA complex shell on the QD surface (as evidenced by our PL data and those in ref.^[35]). As a result, the PL intensity of the as-synthesized PbS QDs decreased gradually when the Pb/S molar ratio was decreased to lower than 10:3. In the case of a 1:1 Pb/S feed molar ratio, as expected, large particles were formed and precipitated out quickly, suggesting that the Pb/S feed molar ratio needs to be larger than 1:1 to avoid uncontrollable growth.

In addition to the Pb/S feed molar ratio described above, the OA/Pb feed molar ratio was also observed to influence the PL properties of the resulting PbS QDs. Here, the concentration of Pb^{2+} ions was fixed at 10 mM and the Pb/S molar ratio was set to 10:3. As shown in Figure 2B, when tuning the OA/Pb molar ratio from 20:10 to 80:10, the PL emission intensity firstly increased then decreased, and it reached a maximum at an OA/Pb molar ratio of 40:10. Meanwhile, we noted that such increase in the OA/Pb feed molar ratio only causes a small redshift in the PL emission peak (ca. 15 nm, from ca. 760 to ca. 775 nm). These experimental results demonstrate that the OA/Pb feed molar ratio plays a more important role in determining the PL emission intensity rather than the PL peak position. Hence, in this study, the precursor OA/Pb/S feed molar ratio of 40:10:3 is optimal for the synthesis of oil-soluble, NIR-emitting PbS QDs.

In this study, we also explored the storage stability of the as-synthesized PbS QDs prepared by using Na_2S as sulfur source to further evaluate the QD quality. As we know, storage stability is important for the potential applications of the QDs. Here, the prepared QD solutions were stored at room temperature in the dark. Temporal evolutions of PL and NIR absorption spectra of PbS QDs during storage are shown in Figure 3. These data show that for the initial seven days, the optical properties (PL emission and absorption) of the QD solution is relatively stable; the PL emission intensity will decrease slowly with prolonged storage time. However, it is worth mentioning that after approximately 30 d of storage at room temperature, the PL emission intensity of the QD dispersions decreased only by about 20%, and no obvious redshift in the PL peak was observed. Hence, the OA-capped PbS QDs prepared by using Na_2S as sulfur source have slightly improved storage stability, as compared to those obtained by using the dangerous bis(trimethylsilyl) sulfide $[(\text{TMS})_2\text{S}]$ as sulfur source.^[19,27] Meanwhile, this result also confirms further that lead sulfide QDs have better chemical stability (air-stable) under ambient conditions, in comparison to phosphide and arsenide QDs,^[12–14] which is important for technical applications.

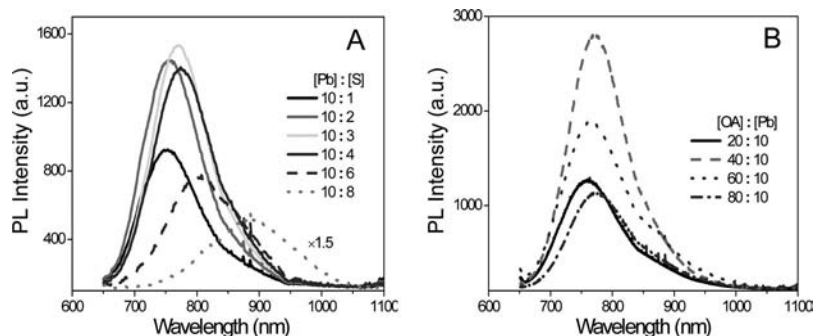


Figure 2. Photoluminescence spectra of OA-capped PbS QDs prepared by using Na_2S as sulfur source, obtained by changing the precursor Pb/S feed molar ratio (A) or the precursor OA/Pb feed molar ratio (B) ($[\text{Pb}^{2+}] = 10 \text{ mM}$).

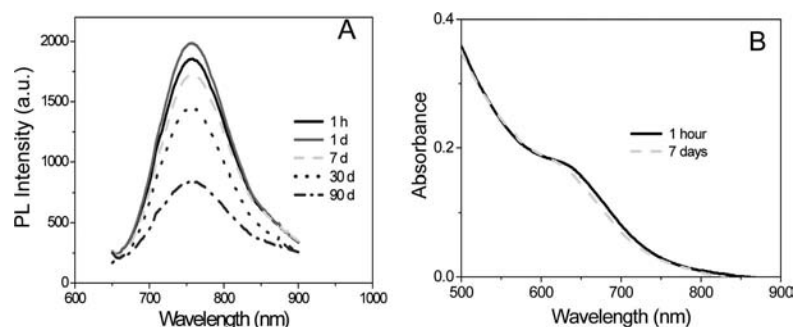


Figure 3. Photoluminescence (A) and absorption (B) spectra of OA-capped PbS QDs monitored at different time intervals. The PbS QDs synthesized at 40 °C with Na₂S as sulfur source and a precursor molar ratio OA/Pb/S of 40:10:3 ([Pb²⁺] = 10 mM) are stored at room temperature in the dark.

Synthesis of OA-Capped PbS QDs by Using Moderately Reactive Thioacetamide as Sulfur Source

In this study, highly luminescent, NIR-emitting, oil-soluble PbS QDs (PL peak: from ca. 750 to ca. 880 nm) with a narrow size distribution were prepared by using Na₂S as sulfur source via a two-phase approach at an *n*-decane/water interface. Sodium sulfide, as a highly reactive sulfur source, will result in a rapid nucleation event. In this case, a larger number of smaller PbS particles are achieved. As proved in previous studies on the two-phase syntheses of CdS and CdSe QDs by An et al.,^[34] the reactivity of anion precursors plays an important and complicated role in affecting the nucleation and growth of the QDs. Here, we noted that there is a significant difference between the synthesis of PbS and those of CdS and CdSe with respect to their influence on the QD growth rate. The growth of PbS QDs is much faster, and can even occur at room temperature, relative to CdS or CdSe QDs.^[26,27] Thus, the role that the activity of the anion precursor plays in the nucleation and growth processes of PbS QDs in our two-phase system and how it can be controlled is the next question to investigate.

The reactivity of an anion precursor depends mainly on its nature. In this case, we used thioacetamide (TAA) and thiourea as sulfur sources (see the Experimental Section for more details) to understand and reveal the influence of the reactivity of the S precursors on the nucleation and growth of PbS QDs. As compared to highly reactive sodium sulfide, TAA and thiourea are moderately reactive and poorly reactive, respectively, according to the report by An and co-workers.^[34] In our two-phase system, when using poorly reactive thiourea as sulfur source, the resulting PbS QDs show very poor near-infrared fluorescence. Therefore, in this work, we study the influence of the reactivity of TAA (moderately reactive) on the synthesis of PbS QDs. Besides the nature of the precursor, the reaction temperature may also play an important role in adjusting the reactivity of anion precursors. So in this part, we further study the effect of the reaction temperature on the reactivity of TAA. The experimental results obtained are shown in Figure 4, where

the (initial) reaction temperatures were set at 60, 65, and 70 °C. The selection of a suitable reaction temperature is based on the thermal decomposition temperature of TAA (about 55 °C in water). The results presented in Figure 4 are as follows:

(1) Using moderately reactive TAA as sulfur precursor will slow down the nucleation rate of the PbS QDs, relative to highly reactive Na₂S. As shown in Figure 4A, at the lower reaction temperature (60 °C), the decomposition rate of TAA is very slow. Under normal pressure, it takes about 35 min for a color change from pale yellow to pale brown to appear. In the following 15–20 min (from 35 min to 50–55 min), the residual TAA decomposes continually to release sulfur anions. As we know, the released sulfur anions could react with Pb cations to form new crystal nuclei of PbS or feed the growth of the formed QDs. Here, the PL peak redshifts from approximately 835 nm to about 895 nm, but the PL spectra do not broaden with reaction time (PL bandwidth ca. 130 nm), which suggests that the decomposition of TAA mainly feeds the QD growth rather than forming new crystal nuclei, according to the QD growth theory reported by Peng et al.^[36] On prolonging the reaction time further (>50–55 min), the TAA is consumed eventually. At this time, the growth of QDs is in conformity with the Ostwald ripening mechanism (the smaller particles dissolve, feeding growth of the bigger nanocrystals), resulting in the broadening of the size distribution. The corresponding PL bandwidth broadens from approximately 130 nm to about 150 nm.

(2) When the reaction temperature is increased to 65 °C, the decomposition rate of TAA and the resulting nucleation and growth rates of PbS QDs all increase. As displayed in Figure 4B, at 65 °C, the time needed for the appearance of a color change from pale yellow to pale brown is shortened to 25 min. Approximately in the next 9 min (from 25 to 34 min), the residual TAA decomposes rapidly and is consumed eventually. As a result, the PbS QDs grow fast. The PL peak redshifts significantly from 800 to 890 nm within approximately 9 min. Meanwhile, the appearance of double peak structures in the PL spectra suggests that, due to the high decomposition rate of TAA and the high growth rate of QDs at 65 °C, some new crystal nuclei of PbS are formed

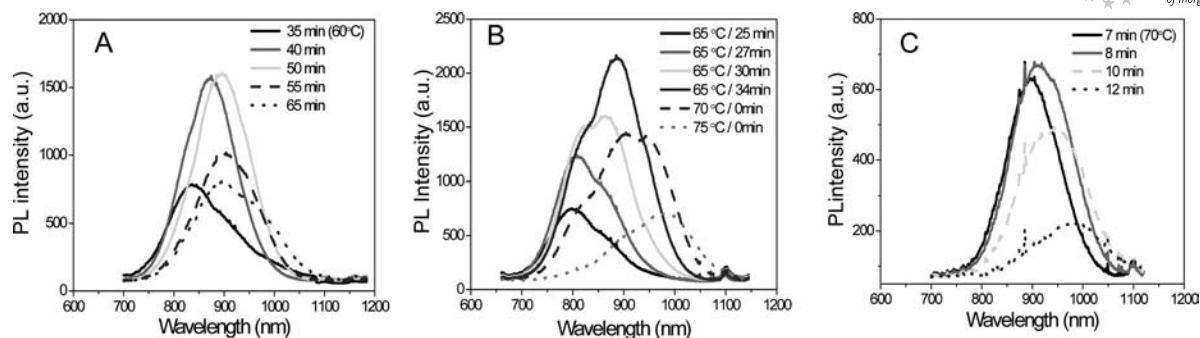


Figure 4. Temporal evolution of the PL spectra of OA-capped PbS QDs prepared with TAA as sulfur source. Quantum dots grown at 60 °C (A), 65 to 75 °C (B), and 70 °C (C). Here, the precursor molar ratio of OA/Pb/S is 40:10:3 ($[\text{Pb}^{2+}] = 10 \text{ mM}$).

besides feeding the growth of the formed QDs,^[37] which results in an accompanying spectral broadening (the PL bandwidth broadens from ca. 140 to ca. 160 nm). Then, we further increased the reaction temperature from 65 °C to 75 °C at a rate of approximately 1 °C/min. During such a temperature increase, the PL peak of the resulting PbS QDs redshifted rapidly from approximately 890 to about 980 nm, and the fwhm (or PL bandwidth) increased further from approximately 160 to about 180 nm upon the action of Ostwald ripening; the corresponding PL emission intensity decreased gradually. It should be mentioned that, at 65 °C or 60 °C, the as-synthesized PbS QDs showed strong NIR fluorescence emission. PL QYs for the most favorable products were determined to be of the order of approximately 35% relative to the standard NIR dye cypate.

(3) As shown in Figure 4C, the decomposition rate of TAA (i.e., the rate of release of the sulfur monomer) and the subsequent nucleation and growth rate of PbS QDs at 70 °C are much faster relative to those at 60 °C and 65 °C. After only approximately 6–7 min, we could observe a color change from pale yellow to brown, which might indicate that at 70 °C, the TAA (sulfur source) is rapidly consumed. In the next 5 min (from 7 to 12 min), the PL peak redshifted fast from 895 to 975 nm; the corresponding PL emission bandwidth broadened rapidly from 130 to 180 nm, as a result of the interaction of the rapid release of sulfur monomer and the “Ostwald ripening” effect. In addition, at the higher reaction temperature (70 °C), the initially formed crystal nuclei of PbS have a large particle size, and the resulting PbS QDs show relatively poor NIR fluorescence (PL QY ca. 10%).

The experimental results described above fully confirm that the reactivity of water-soluble sulfur precursors plays an important and complicated role in affecting the nucleation and growth of the oil-soluble PbS QDs in a two-phase system; by controlling the reaction temperature, the decomposition rate of TAA can also be adjusted. In particular, with increasing reaction temperature, the decomposition rate of TAA and the nucleation and growth rates of PbS QDs all increase, but such changes are not uniform. At lower reaction temperatures (60–65 °C), the decomposition rate of TAA and the nucleation and growth rates of QDs all are low, which results in the overlap of the nucleation

process with the growth process to different degrees. At 60 °C, a slow nucleation (because of a slow decomposition of TAA) does not lead to polydisperse nanocrystals, since the growth is also slow,^[34] and the PL bandwidth is stable at approximately 130 nm before the TAA is exhausted. On increasing the reaction temperature to 65 °C, the growth rate of PbS QDs might improve more than the decomposition rate of TAA and the nucleation rate. As a result, the PL spectra display double peak structures (the PL bandwidth is broadened to ca. 160 nm), presumably due to the appearance of two main QD populations of slightly different (and approximate) average sizes,^[37] caused by the single nucleation and the fast growth of QDs. When the TAA was exhausted, the PbS QDs grew with further redshifting and broadening of the PL spectra upon the action of Ostwald ripening. At 70 °C, the decomposition rate of TAA and the nucleation and growth rates of PbS QDs all increase greatly. The rapid decomposition of TAA could lead to the rapid formation of large crystal nuclei, and the formed PbS QDs exhibit relatively unfavorable optical properties.

We further explored the storage stability of the resulting PbS QDs prepared by using TAA as sulfur source: the QDs synthesized at 65 °C were stored in the synthesis medium at room temperature. During the storage, the PL and absorption spectra were measured at time intervals spanning up to 30 d, and the results are shown in Figure 5. The initial wide PL spectrum (bandwidth, ca. 160 nm) clearly indicates that the size distribution of the QD sample is broad. With increasing storage time, the PL spectrum sharpens and redshifts gradually, suggesting a spontaneous narrowing of the particle size distribution and an accompanied increase in average particle size. In the case of PbS nanocrystals, the self-focusing of the particle size after the reaction is not uncommon, which has been reported by Hines and Scholes.^[19] They attribute the size focusing to the digestive ripening of PbS nanocrystals. Digestive ripening occurs when larger particles break apart and smaller particles increase in size until a uniform size distribution is achieved. Meanwhile, the spectral feature blueshifts, and the average particle size decreases. Hence, digestive ripening is different from Ostwald ripening, which commonly results in the defocusing of the size distribution and an accompanying red-shift in the PL emission spectra.

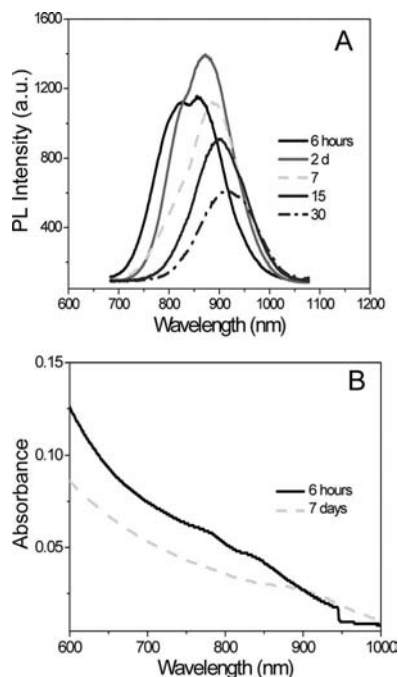


Figure 5. PL (A) and absorption (B) spectra of a single *n*-decane solution of OA-capped PbS QDs measured at different time intervals. The PbS QDs synthesized at 65 °C by using TAA as sulfur source are stored at room temperature in the dark; the precursor molar ratio of OA/Pb/S was 40:10:3 ($[\text{Pb}^{2+}] = 10 \text{ mM}$).

In our experiments, we observed the sharpening and red-shifting of the PL spectrum simultaneously, as shown in Figure 5A. Therefore, in this case, the focusing of the particle size could not be rationally attributed to the digestive ripening of PbS nanocrystals, as observed by Hines et al.^[19] By analyzing the experimental results, we consider that, in this two-phase system, with moderately reactive TAA as sulfur source, at 65 °C, the decomposition of sulfur precursor and the nucleation and growth of the PbS QDs occur simultaneously at the initial stage, resulting in a broad particle size distribution (Figure 4B). When the as-prepared relatively polydisperse PbS QDs (confirmed by TEM analysis) are further stored in the synthesis medium at room temperature, the smaller particles begin to dissolve gradually, feeding the growth of the bigger nanocrystals. However, unlike those occurring generally at high reaction temperature, this process is very slow at room temperature and tends to be thermodynamically stable. As a result, the size distribution of the PbS QDs becomes narrower, and this is accompanied by gradual redshifts of the optical spectra.

Here, it should be mentioned that generally, the PL emission intensity of the PbS QDs decreased gradually during the storage, as presented in Figure 5A. After storage for approximately 30 d, the corresponding photoemission intensity was reduced by about 50%, suggesting a relatively poor storage stability compared to that of the PbS QDs obtained by using Na_2S as sulfur source. However, in our experiments, we noted that it is easy to precipitate the as-synthesized PbS QDs in *n*-decane solution with methanol

or ethanol, and it is also easy to isolate them by centrifugation and decantation; the obtained purified QD samples (that can be redispersed in *n*-decane) will show more favorable storage stability than the corresponding QD solution, regardless of whether they were obtained by using Na_2S or TAA as sulfur source.

When using poorly reactive thiourea as sulfur source, the resulting PbS QDs will exhibit very poor near-infrared fluorescence (data not shown), and the reaction has a poor reproducibility. Each time, the size and PL properties of PbS QDs might be different at the same temperature and reaction time. These experimental results are greatly different from those of the CdS or CdSe QDs, where poorly reactive thiourea was found to be more favorable for the formation of QDs.^[34] This difference might be attributed to the high decomposition temperature of thiourea and the high growth rate of PbS QDs. Specifically, the decomposition temperature of thiourea in water is high, close to 100 °C. At this reaction temperature, the growth rate of PbS QDs is very fast (as compared to CdS QDs,^[34] the growth of PbS QDs is much faster, it could even occur at room temperature), and the high reaction temperature is also unfavorable for preparing highly luminescent PbS QDs as shown in Figure 1B. Therefore, it is difficult to improve the size controllability and PL properties of PbS QDs by changing the reaction parameters and using poorly reactive thiourea as sulfur source. These experimental results enhance our understanding of the relation between the reactivity of water-soluble anion precursors and the QD synthesis in a two-phase system: the selection of water-soluble anion precursors for the QD synthesis depends on their reactivity and the rate of growth of the QDs. That is to say, if the growth rate of QDs is high (as in the present study), we should select highly reactive water-soluble anion precursors; otherwise, the situation is the converse (as in the report of An et al.^[34]).

Morphological and Structural Characterizations of As-Synthesized OA-Capped PbS QDs

In this study, transmission electron microscopy (TEM) and powder XRD were employed to characterize the morphology and crystal structure of oil-soluble PbS QDs synthesized by a two-phase approach, using highly reactive water-soluble Na_2S and moderately reactive thioacetamide (TAA) as sulfur sources. The experimental results are shown in Figures 6 and 7, respectively. As presented in Figure 6A, the PbS QDs ($\lambda_{\text{em}} = 800 \text{ nm}$) obtained by using highly reactive Na_2S as sulfur source appear as well-separated nearly spherical particles with good monodispersity (the average size is ca. 4 nm). Figure 6B is a typical TEM image of the PbS QDs ($\lambda_{\text{em}} = 808 \text{ nm}$) grown at 65 °C obtained by using TAA as sulfur source, showing that these QDs have a slightly poorer size uniformity (and monodispersity), as compared to the PbS QDs obtained with Na_2S as sulfur source (generally, the particle size of PbS QDs produced from thioacetamide is larger than that obtained

from Na_2S , because thioacetamide produces long-wavelength-emitting PbS). The inset HRTEM images (bottom) reveal that the as-prepared OA-capped PbS QDs obtained from two kinds of differently reactive sulfur sources are all well-crystallized. The lattice spacing, as labeled in the HRTEM images, is approximately 0.29 nm, corresponding to the (200) plane of the cubic structure of PbS.^[25–27] The selected area electron diffraction (SAED) patterns (top)

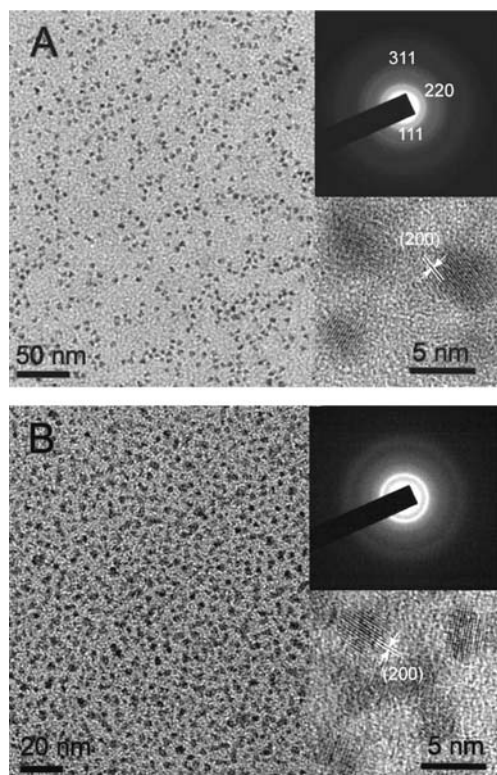


Figure 6. (A) Typical TEM image of OA-capped PbS QDs ($\lambda_{\text{em}} = 800$ nm) with an OA/Pb/S ratio of 40:10:3 obtained by using highly reactive Na_2S as sulfur source. (B) Typical TEM image of the PbS QDs ($\lambda_{\text{em}} = 808$ nm) grown at 65 °C with a OA/Pb/S ratio of 40:10:3 by using moderately reactive thioacetamide as sulfur source. Insets are the corresponding SAED pattern (top) and high-resolution TEM image (bottom) of the PbS QDs.

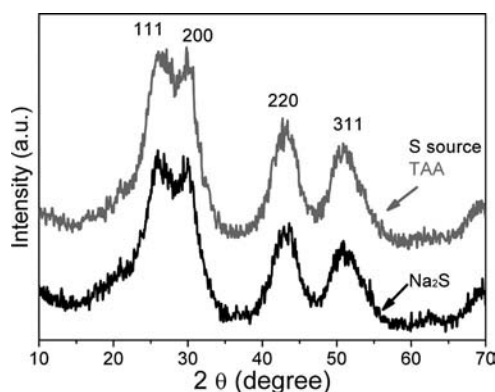


Figure 7. Typical powder XRD patterns of the two OA-capped PbS QD samples (shown in panels A and B of Figure 6) supported on a glass slide. The diffraction peaks are indexed.

also prove the QDs to be crystalline. The three lattice spacings calculated from the diffraction rings are 0.34, 0.21, and 0.18 nm, corresponding to the reported d spacings for lattice planes (111), (220), and (311) of cubic PbS. Figure 7 shows the typical powder XRD patterns of the two OA-capped PbS QD samples (shown in Figure 6A and B) supported on a glass slide. The XRD patterns also indicate that these oil-soluble PbS QDs have a cubic crystal structure. It is clear that the diffraction peaks are broader than those in previous reports,^[21–25] implying a smaller QD size. Thus, the experimental results from XRD measurement are rather consistent with HRTEM imaging and SAED analysis, confirming the uniform cubic structure and the extremely small size of the produced PbS QDs.

Conclusions

A facile and low-cost two-phase approach under mild conditions has been developed to prepare high-quality hydrophobic PbS QDs that offer size-tunable fluorescence emission in the wide NIR range of approximately 750–1000 nm, by using differently reactive water-soluble Na_2S and TAA as sulfur sources. (1) Using highly reactive Na_2S as sulfur precursor, small PbS QDs with a narrow size distribution, which show strong photoluminescence (PL QY up to 40%), are prepared by our two-phase approach; the PL peak position can be tuned between 750 and 880 nm. Moreover, systematic investigation has been performed on the synthesis parameters affecting the formation of PbS QDs, including the reaction temperature, the precursor Pb/S molar ratio, the precursor OA/Pb molar ratio, and the storage stability. In general, these factors play crucial roles leading to high-quality PbS QDs. (2) Moderately reactive TAA was used further as sulfur precursor to explore the influence of the reactivity of water-soluble sulfur sources on the synthesis of oil-soluble NIR-emitting PbS QDs in our two-phase system. It was found that the decomposition of TAA and the accompanying nucleation and growth of PbS QDs strongly depends on the applied synthesis temperature. A reaction temperature between 60 and 65 °C is favorable for the formation of highly luminescent PbS QDs (PL QY up to 35%) that show long-wavelength fluorescence emission (the PL peak position can be tuned from 800 to 980 nm). Hence, these experimental results confirm fully that the reactivity of the anion precursors plays an important and unique role in determining the nucleation and growth of QDs in the two-phase synthesis system. In addition, we characterized the morphology and crystal structure of the resulting PbS QDs by (high-resolution) TEM and SAED, and powder XRD. The obtained experimental results confirm fully that the produced oil-soluble NIR-emitting PbS QDs have a cubic crystal structure and extremely small size.

Currently, our efforts are directed to two main investigations. One is to place these oil-soluble PbS QDs into the hydrophobic cores of nanoscale micelles (potential drug carriers) for evaluating their in vivo tumor-specific tar-

getting, by using the NIR imaging system constructed in our lab;^[7b,7c] the other is to seek a simple and efficient procedure for transferring oil-soluble PbS QDs into water. These studies are all of great importance for future technical applications of oil-soluble PbS QDs. (**Caution:** Although the toxicity of PbS QDs may be lower than those of Cd-, Hg-, Te-, and Se-based ones, *in vivo* biomedical experiments of these QDs should be limited to mice or other animals.)

Experimental Section

Chemicals: Lead(II) acetate trihydrate (99+%), oleic acid (99%), *n*-decane (99%), Na₂S·9H₂O (98+%), thioacetamide (TAA, 99.5%), and thiourea (99%) were of analytical grade and used as received. The water used in all experiments had a resistivity higher than 18.2 MΩ·cm.

Synthesis of OA-Capped PbS QDs by Using Various Water-Soluble Anion Precursors: The typical two-phase synthetic approach to oil-soluble near-infrared-emitting PbS QDs can be divided into two steps (see Figure 8A): first, the Pb-precursor solution is prepared; then, the *n*-decane solution of lead precursor is mixed with an aqueous solution of sulfur precursor, such as Na₂S, thioacetamide (TAA), or thiourea, at the desired temperature. Thus, NIR-emitting

PbS QDs are prepared. A scheme in Figure 8B which illustrates the proposed mechanism for the formation of NIR-emitting oil-soluble PbS QDs by using water-soluble Na₂S, TAA (and thiourea) as sulfur sources with different reactivity. Both nucleation and growth of QDs occur at the interface of the two liquid phases (i.e., *n*-decane and water).^[29,30]

Preparation of the Pb Precursor Solution: A typical reaction was performed by placing lead acetate (38 mg), oleic acid (0.13 mL), and *n*-decane (10 mL) in a continuously stirred flask and then heating the mixture at 130 °C for 20 min until an optically clear precursor solution of lead oleate was obtained. Finally, the solution was cooled to the desired temperature (for example, 40 °C for the synthesis with Na₂S as sulfur precursor). This reaction was run under a nitrogen atmosphere to prevent oxidation of the oxygen-sensitive oleic acid.

Synthesis of PbS QDs with Na₂S as Sulfur Source: When the above lead oleate precursor solution was cooled to 40 °C, an aqueous solution (5 mL, 6 mM) of Na₂S prepared freshly was added dropwise to the reaction flask whilst stirring. Immediately, the upper organic phase turned from pale yellow to dark-brown within about one minute, which indicates that the formation of PbS QDs occurred rapidly in a two-phase synthesis system when using highly reactive Na₂S as sulfur source. Subsequently, the system was stirred further at 40 °C for 5 min. Finally, the solution was cooled to room temperature for UV/Vis absorbance and photoluminescence (PL) measurements without any size sorting. In this part, we investigated further the effects of the temperature, the precursor Pb/S molar ratio, the precursor OA/Pb molar ratio, and the storage time on the synthesis of PbS.

Synthesis of PbS QDs with Thioacetamide as Sulfur Source: When the freshly prepared lead oleate precursor solution was cooled to 60 °C (or 65 °C or 70 °C), a solution of moderately reactive thioacetamide (5 mL, 6 mM) in water was injected into the reaction flask whilst stirring. Next, the reaction mixture was kept at 60 °C (or 65 °C or 70 °C) for promoting the nucleation and growth of PbS QDs. Aliquots were taken at different time intervals, and UV/Vis absorbance and PL spectra were recorded for each aliquot. In this part, we investigated the influence of the reaction temperature on the reactivity (or decomposition) of TAA and the resultant nucleation and growth of PbS QDs.

Characterization: An S2000 eight-channel optical fiber spectrophotometer (Ocean Optics corporation, America) and a broadband light source ($\lambda_{\text{ex}} \approx 610$ nm) (X-Cite Series 120Q, Lumen Dynamics Group Inc., Canada) were utilized for the detection of fluorescence spectra. A 754-PC UV/Vis spectrophotometer (JingHua technological instrument corporation, Shanghai, China) was used for the measurement of UV/Vis spectra. All optical measurements were performed at room temperature. PL quantum yields (QY) of PbS QDs in *n*-decane were calculated by comparing their integrated emission to that of a solution of cypate in 20% aq. DMSO (the absorption and PL emission peaks of cypate are at 790 nm and 810 nm, respectively; the PL QY is 12%) supplied by Samuel Achilefu (Department of radiology, Washington University at St. Louis, USA).^[38] A JEM-2100 transmittance electron microscope (JEOL, Japan) operated at 200 kV was used to evaluate the morphology and crystal structure of quantum dots. Powder XRD measurements were carried out using a Philips X'Pert PRO X-ray diffractometer ($\lambda = 1.54178$ Å). XRD samples were prepared by concentrating a drop of the obtained concentrated QD ethanol suspension on a glass plate.

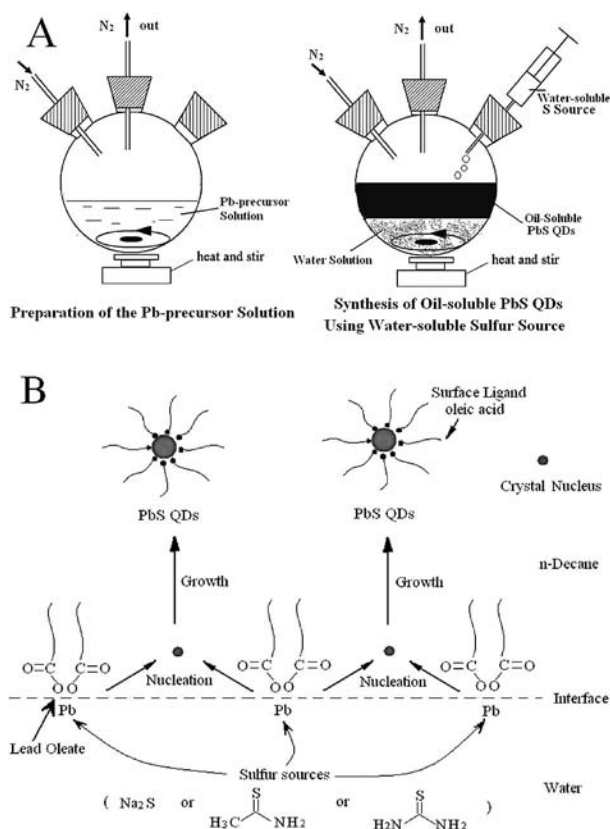


Figure 8. (A) Schematic presentation of the two-phase synthetic route to oil-soluble PbS QDs by using water-soluble Na₂S, thioacetamide (TAA), and thiourea as sulfur sources: preparation of the Pb precursor solution; synthesis of oil-soluble PbS QDs by using the water-soluble sulfur source. (B) A proposed mechanism for forming oil-soluble PbS QDs by using various water-soluble sulfur sources. Both nucleation and growth of QDs only occur at the interface of the two liquid phases (i.e., *n*-decane and water).

Acknowledgments

This work was financially supported by the National Natural Science Foundation of China [No. 30800257 (Youth Science Funds), No. 30970776, No. 31050110123, and No. 81071194]. In addition, here we express our sincere thanks to Prof. Samuel Achilefu (Department of Radiology, Washington University at St. Louis) for supplying the near-infrared fluorescent dye cypate.

- [1] a) M. Nirmal, L. Brus, *Acc. Chem. Res.* **1999**, *32*, 407–414; b) C. B. Murray, C. R. Kagan, M. G. Bawendi, *Annu. Rev. Mater. Sci.* **2000**, *30*, 545–610.
- [2] a) A. L. Rogach, N. Gaponik, J. M. Lupton, C. Berton, D. E. Gallardo, S. Dunn, N. L. Pira, M. Paderi, P. Repetto, S. G. Romanov, C. O'Dwyer, C. M. S. Torres, A. Eychmüller, *Angew. Chem. Int. Ed.* **2008**, *47*, 6538–6549; b) W. U. Huynh, J. J. Dittmer, A. P. Alivisatos, *Science* **2002**, *295*, 2425–2427; c) X. Michalet, F. F. Pinaud, L. A. Bentolila, J. M. Tsay, S. Doose, J. J. Li, G. Sundaresan, A. M. Wu, S. S. Gambhir, S. Weiss, *Science* **2005**, *307*, 538–544.
- [3] a) C. B. Murray, D. J. Norris, M. G. Bawendi, *J. Am. Chem. Soc.* **1993**, *115*, 8706–8715; b) D. V. Talapin, A. L. Rogach, A. Kornowski, M. Haase, H. Weller, *Nano Lett.* **2001**, *1*, 207–211; c) J. J. Li, Y. A. Wang, W. Guo, J. C. Keay, T. D. Mishima, M. B. Johnson, X. G. Peng, *J. Am. Chem. Soc.* **2003**, *125*, 12567–12575; d) R. E. Bailey, S. M. Nie, *J. Am. Chem. Soc.* **2003**, *125*, 7100–7106.
- [4] a) Y. Wang, Z. Tang, M. A. Correa-Duarte, I. Pastoriza-Santos, M. Giersig, N. A. Kotov, L. M. Liz-Marzán, *J. Phys. Chem. B* **2004**, *108*, 15461–15469; b) N. Gaponik, A. L. Rogach, *Phys. Chem. Chem. Phys.* **2010**, *12*, 8685–8693.
- [5] a) E. H. Sargent, *Adv. Mater.* **2005**, *17*, 515–522; b) A. L. Rogach, A. Eychmüller, S. G. Hickey, S. V. Kershaw, *Small* **2007**, *3*, 536–557; c) J. V. Frangioni, *Curr. Opin. Chem. Biol.* **2003**, *7*, 626–634.
- [6] a) S. Kim, Y. T. Lim, E. G. Soltész, A. M. De Grand, J. Lee, A. Nakayama, J. A. Parker, T. Mihaljevic, R. G. Laurence, D. M. Dor, L. H. Cohn, M. G. Bawendi, J. V. Frangioni, *Nat. Biotechnol.* **2004**, *22*, 93–97; b) X. H. Gao, Y. Y. Cui, R. M. Levenson, L. W. K. Chung, S. M. Nie, *Nat. Biotechnol.* **2004**, *22*, 969–976; c) E. B. Voura, J. K. Jaiswal, H. Mattoussi, S. M. Simon, *Nat. Med.* **2004**, *10*, 993–998.
- [7] a) M. Y. Berezin, S. Achilefu, *Chem. Rev.* **2010**, *110*, 2641–2684; b) J. Zhang, H. Chen, L. Xu, Y. Q. Gu, *J. Controlled Release* **2008**, *131*, 34–40; c) J. Zhang, D. W. Deng, Z. Y. Qian, F. Liu, X. Y. Chen, L. X. An, Y. Q. Gu, *Pharm. Res.* **2010**, *27*, 46–55.
- [8] a) A. L. Rogach, T. Franzl, T. A. Klar, J. Feldmann, N. Gaponik, V. Lesnyak, A. Shavel, A. Eychmüller, Y. P. Rakovich, J. F. Donegan, *J. Phys. Chem. C* **2007**, *111*, 14628–14637; b) J. M. Tsay, M. Pflughoeft, L. A. Bentolila, S. Weiss, *J. Am. Chem. Soc.* **2004**, *126*, 1926–1927.
- [9] a) S. Kim, B. Fisher, H. J. Eisler, M. G. Bawendi, *J. Am. Chem. Soc.* **2003**, *125*, 11466–11467; b) K. Yu, B. Zaman, S. Romanova, D. S. Wang, J. A. Ripmeester, *Small* **2005**, *1*, 332–338; c) B. A. Kairdolf, A. M. Smith, S. M. Nie, *J. Am. Chem. Soc.* **2008**, *130*, 12866–12867.
- [10] H. F. Qian, C. Q. Dong, J. L. Peng, X. Qiu, Y. H. Xu, J. C. Ren, *J. Phys. Chem. C* **2007**, *111*, 16852–16857.
- [11] a) M. T. Harrison, S. V. Kershaw, A. L. Rogach, A. Kornowski, A. Eychmüller, H. Weller, *Adv. Mater.* **2000**, *12*, 123–125; b) M. V. Kovalenko, E. Kaufmann, D. Pachinger, J. Roither, M. Huber, J. Stangl, G. Hesser, F. Schäffler, W. Heiss, *J. Am. Chem. Soc.* **2006**, *128*, 3516–3517.
- [12] a) J. H. Gao, K. Chen, R. G. Xie, J. Xie, Y. J. Yan, Z. Cheng, X. G. Peng, X. Y. Chen, *Bioconjugate Chem.* **2010**, *21*, 604–609; b) J. H. Gao, K. Chen, R. G. Xie, J. Xie, S. Lee, Z. Cheng, X. G. Peng, X. Y. Chen, *Small* **2010**, *6*, 256–261.
- [13] a) S. W. Kim, J. P. Zimmer, S. Ohnishi, J. B. Tracy, J. V. Frangioni, M. G. Bawendi, *J. Am. Chem. Soc.* **2005**, *127*, 10526–10532; b) P. M. Allen, W. H. Liu, V. P. Chauhan, J. Lee, A. Y. Ting, D. Fukumura, R. K. Jain, M. G. Bawendi, *J. Am. Chem. Soc.* **2010**, *132*, 470–471.
- [14] a) R. G. Xie, X. G. Peng, *J. Am. Chem. Soc.* **2009**, *131*, 10645–10651; b) D. W. Lucey, D. J. MacRae, M. Furis, Y. Sahoo, A. N. Cartwright, P. N. Prasad, *Chem. Mater.* **2005**, *17*, 3754–3762.
- [15] a) P. M. Allen, M. G. Bawendi, *J. Am. Chem. Soc.* **2008**, *130*, 9240–9241; b) M. G. Panthani, V. Akhavan, B. Goodfellow, J. P. Schmidtke, L. Dunn, A. Dodabalapur, P. F. Barbara, B. A. Korgel, *J. Am. Chem. Soc.* **2008**, *130*, 16770–16777; c) R. G. Xie, M. Rutherford, X. G. Peng, *J. Am. Chem. Soc.* **2009**, *131*, 5691–5697.
- [16] a) S. L. Castro, S. G. Bailey, R. P. Raffaele, K. K. Banger, A. F. Hepp, *Chem. Mater.* **2003**, *15*, 3142–3147; b) B. Koo, R. N. Patel, B. Korgel, *J. Am. Chem. Soc.* **2009**, *131*, 3134–3135.
- [17] a) H. Nakamura, W. Kato, M. Uehara, K. Nose, T. Omata, S. Otsuka-Yao-Matsuo, M. Miyazaki, H. Maeda, *Chem. Mater.* **2006**, *18*, 3330–3335; b) L. Li, T. J. Daou, I. Texier, T. K. C. Tran, Q. L. Nguyen, P. Reiss, *Chem. Mater.* **2009**, *21*, 2422–2429; c) T. Pons, E. Pic, N. Lequeux, E. Cassette, L. Bezdetnaya, F. Guillemin, F. Marchal, B. Dubertret, *ACS Nano* **2010**, *4*, 2531–2538.
- [18] T. Torimoto, T. Adachi, K. Okazaki, M. Sakuraoaka, T. Shibayama, B. Ohtani, A. Kudo, S. Kuwabata, *J. Am. Chem. Soc.* **2007**, *129*, 12388–12389.
- [19] M. A. Hines, G. D. Scholes, *Adv. Mater.* **2003**, *15*, 1844–1849.
- [20] a) S. M. Lee, Y. W. Jun, S. N. Cho, J. W. Cheon, *J. Am. Chem. Soc.* **2002**, *124*, 11244–11245; b) D. B. Kuang, A. W. Xu, Y. P. Fang, H. Q. Liu, C. Frommen, D. Fenske, *Adv. Mater.* **2003**, *15*, 1747–1750; c) J. Zhu, H. Peng, C. K. Chan, K. Jarausch, X. F. Zhang, Y. Cui, *Nano Lett.* **2007**, *7*, 1095–1099; d) Y. K. A. Lau, D. J. Chernak, M. J. Bierman, S. Jin, *J. Am. Chem. Soc.* **2009**, *131*, 16461–16471; R. Jin, G. Chen, Q. Wang, J. Pei, G. Wang, L. Wang, *Eur. J. Inorg. Chem.* **2010**, 5700–5708.
- [21] L. Bakueva, I. Gorelikov, S. Musikhin, X. S. Zhao, E. H. Sargent, E. Kumacheva, *Adv. Mater.* **2004**, *16*, 926–929.
- [22] D. W. Deng, W. C. Zhang, X. Y. Chen, F. Liu, J. Zhang, Y. Q. Gu, J. M. Hong, *Eur. J. Inorg. Chem.* **2009**, 3440–3446.
- [23] B. Hennequin, L. Turianska, T. Ben, A. M. Beltrán, S. I. Molina, M. Li, S. Mann, A. Patané, N. R. Thomas, *Adv. Mater.* **2008**, *20*, 3592–3596.
- [24] K. A. Abel, J. Shan, J. C. Boyer, F. Harris, F. C. J. M. van Veggel, *Chem. Mater.* **2008**, *20*, 3794–3796.
- [25] a) L. Cademartiri, E. Montanari, G. Calestani, A. Migliori, A. Guagliardi, G. A. Ozin, *J. Am. Chem. Soc.* **2006**, *128*, 10337–10346; b) I. Moreels, K. Lambert, D. Smeets, D. De Muynck, T. Nollet, J. C. Martins, F. Vanhaecke, A. Vantomme, C. Deleue, G. Allan, Z. Hens, *ACS Nano* **2009**, *3*, 3023–3030; c) H. G. Zhao, D. F. Wang, T. Zhang, M. Chaker, D. L. Ma, *Chem. Commun.* **2010**, 5301–5303.
- [26] a) J. H. Warner, E. Thomsen, A. R. Watt, N. R. Heckenberg, H. Rubinsztein-Dunlop, *Nanotechnology* **2005**, *16*, 175–179; b) M. J. Fernée, P. Jensen, H. Rubinsztein-Dunlop, *ACS Nano* **2009**, *3*, 2731–2739.
- [27] T. Y. Liu, M. J. Li, J. Y. Ouyang, M. B. Zaman, R. B. Wang, X. H. Wu, C. S. Yeh, Q. Lin, B. Yang, K. Yu, *J. Phys. Chem. C* **2009**, *113*, 2301–2308.
- [28] N. R. Jana, X. G. Peng, *J. Am. Chem. Soc.* **2003**, *125*, 14280–14281.
- [29] D. C. Pan, S. C. Jiang, L. J. An, B. Z. Jiang, *Adv. Mater.* **2004**, *16*, 982–985.
- [30] D. C. Pan, Q. Wang, S. C. Jiang, X. L. Ji, L. J. An, *Adv. Mater.* **2005**, *17*, 176–179.
- [31] D. C. Pan, N. N. Zhao, Q. Wang, S. C. Jiang, X. L. Ji, L. J. An, *Adv. Mater.* **2005**, *17*, 1991–1995.
- [32] a) N. N. Zhao, D. C. Pan, W. Nie, X. L. Ji, *J. Am. Chem. Soc.* **2006**, *128*, 10118–10124; b) D. C. Pan, Q. Wang, L. J. An, *J. Mater. Chem.* **2009**, *19*, 1063; c) T. D. Nguyen, T. O. Do, *J. Phys. Chem. C* **2009**, *113*, 11204–11214.

- [33] M. Brust, M. Walker, D. Bethell, D. J. Schiffrin, R. Whyman, *J. Chem. Soc., Chem. Commun.* **1994**, 7, 801–802.
- [34] D. C. Pan, Q. Wang, S. C. Jiang, X. L. Ji, L. J. An, *J. Phys. Chem. C* **2007**, *111*, 5661–5666.
- [35] J. Jasieniak, P. Mulvaney, *J. Am. Chem. Soc.* **2007**, *129*, 2841–2848.
- [36] a) X. G. Peng, J. Wickham, A. P. Alivisatos, *J. Am. Chem. Soc.* **1998**, *120*, 5343–5344; b) Z. Peng, X. G. Peng, *J. Am. Chem. Soc.* **2001**, *123*, 183–184.
- [37] H. G. Zhao, M. Chaker, D. L. Ma, *J. Phys. Chem. C* **2009**, *113*, 6497–6504.
- [38] Y. P. Ye, S. Bloch, B. G. Xu, S. Achilefu, *Bioconjugate Chem.* **2008**, *19*, 225–234.

Received: January 6, 2011
Published Online: April 8, 2011